analytical chemistry

Letter

Cite This: Anal. Chem. XXXX, XXX, XXX−XXX

pubs.acs.org/ac

Label-Free and Immobilization-Free Electrochemical Magnetobiosensor for Sensitive Detection of 5-Hydroxymethylcytosine in Genomic DNA

Lin Cui,[‡] Juan Hu,[‡] Meng Wang,[‡] Chen-chen Li,[‡] and Chun-yang Zhang*

College of Chemistry, Chemical Engineering and Materials Science, Collaborative Innovation Center of Functionalized Probes for Chemical Imaging in Universities of Shandong, Key Laboratory of Molecular and Nano Probes, Ministry of Education, Shandong Provincial Key Laboratory of Clean Production of Fine Chemicals, Shandong Normal University, Jinan, Shandong 250014, PR China

Supporting Information

ABSTRACT: DNA 5-hydroxymethylcytosine (5-hmC) is an important epigenetic biomarker for tumorigenesis, and the loss of 5-hmC levels is associated with leukemia and melanoma cancers. However, it is a great challenge to discriminate 5-hmC from 5-methylcytosine (5-mC) using the conventional bisulfite conversion methods. Herein, we report a label-free and immobilization-free electrochemical magnetobiosensor for sensitive quantification of 5-hmC in genomic DNA based on a dual signal amplification strategy coupled with terminal deoxynucleotidyl transferase (TDT) enzymatic amplification and Ru(III) redox cycling. This screen-printed carbon electrode (SPCE)-based electrochemical magnetobiosensor shows distinct advantages of having low cost and simple fabrication and being label-free, immobilization-free, PCR-free, and radioactive-free. It exhibits high sensitivity with a detection limit of as low as 9.06 fM and a large dynamic range from 0.01 to 1000 pM. Importantly, this biosensor can discriminate 5-hmC from cytosine and 5-mC, and it can successfully detect 5-hmC in live cells.

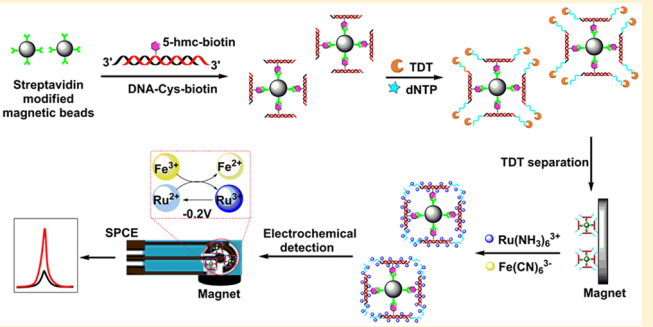

Epigenetic modifications play a crucial role in cellular processes, gene expression, and evolutionary development.[1] DNA 5-hydroxymethylcytosine (5-hmC) is an important epigenetic modification and an intermediate in an active DNA demethylation pathway,[2−4] and it can be catalyzed by oxidation from genomic 5-methylcytosine (5-mC) by ten-eleven translocation (TET) family dioxygenases.[5−8] The 5-hmC level is significantly reduced in cancers and particularly enriched in the brain in mice and humans, suggesting its critical role in tumorigenesis.[2−4] Consequently, accurate quantification of 5-hmC in DNA is essential to the study of the methylation and demethylation mechanism.

In contrast to the 5-mC assay,[9] the accurate quantification of 5-hmC remains a great challenge due to its relatively low abundance and similarity to the abundant 5-mC. The bisulfite sequencing method is regarded as a gold standard for the 5-mC assay, but it suffers from intrinsic drawback of no discrimination between 5-mC and 5-hmC. Alternatively, various methods have been developed for the 5-hmC assay in genomic DNA, such as single-molecule real-time (SMRT) sequencing,[10] liquid chromatography/tandem mass spectrometry (LC/MS-MS),[11] high-performance liquid chromatography (HPLC),[5] thin layer chromatography (TLC),[12,13] enzymatic radioactive glycosylation labeling,[14] and immunoassay.[15−17] These methods can effectively distinguish 5-hmC from 5-mC, but they require the additional fluorescent tags for SMRT, complex and exorbitantly expensive instruments for LC/MS-MS and HPLC, radiolabeled nucleotides and UDP−glucose substrates for TLC and radioactive glycosylation labeling, relatively poor sensitivity for immunoassay, and poor accuracy for TLC.[18] Therefore, it is highly desirable to develop a rapid and simple method for accurate quantification of 5-hmC in genomic DNA.

Due to the advantages of low cost, portability, and high sensitivity, electrochemical biosensors[19,20] based on the enzymatic modification have been used for the detection of low-abundance 5-hmC (pM).[18,21] However, the enzymatic modification-based methods[22,23] require expensive enzymes with restricted recognition motifs, the synthesis of analogues of enzyme cofactors/substrates, and the multiple steps for nucleobase modification. To overcome these limitations, an electrogenerated chemiluminescence (ECL) biosensor has been developed to quantify 5-hmC DNA based on specific oxidation of 5-hmC to 5-formylcytosine (5-fC) by $KRuO_4$ and subsequent labeling with ECL emission molecular *N*-(4-aminobutyl)-*N*-ethylisoluminol (ABEI).[24] Recently, the Bayley

Received: October 11, 2018
Accepted: December 27, 2018
Published: December 27, 2018

DOI: 10.1021/acs.analchem.8b04663
Anal. Chem. XXXX, XXX, XXX−XXX

group[25] and Wu et al.[26] reported an alternative approach in which 5-hmC was one-step chemically modified with biotin in situ, enabling the enrichment of rare 5-hmC-containing sequences and the identification with a protein nanopore. However, these methods are only demonstrated as a proof of concept, and they are not applied for the detection of 5-hmC in genomic DNA.

In this research, we report a label-free electrochemical magnetobiosensor for accurate quantification of 5-hmC in genomic DNA based on a dual signal amplification strategy coupled with terminal deoxynucleotidyl transferase (TDT) and Ru(III) redox cycling. Taking advantage of the screen-printed carbon electrode (SPCE)-based electrochemical magnetobiosensing, this biosensor can sensitively quantify 5-hmC with a detection limit of as low as 9.06 fM without the involvement of the immobilization of DNA on the electrode.[27,28] Importantly, this biosensor can be applied for accurate quantification of 5-hmC in HeLa cells and HEK 293T cells, and it offers a good discrimination toward cytosine, 5-methylcytosine, and 5-hydroxymethylcytosine.

The principle of the 5-hmC assay is illustrated in Scheme 1. The hybridization of 5-hmC ssDNA with the complementary

Scheme 1. Schematic Illustration of a Label-Free and Immobilization-Free Electrochemical Magnetobiosensor for 5-hmC Assay[a]

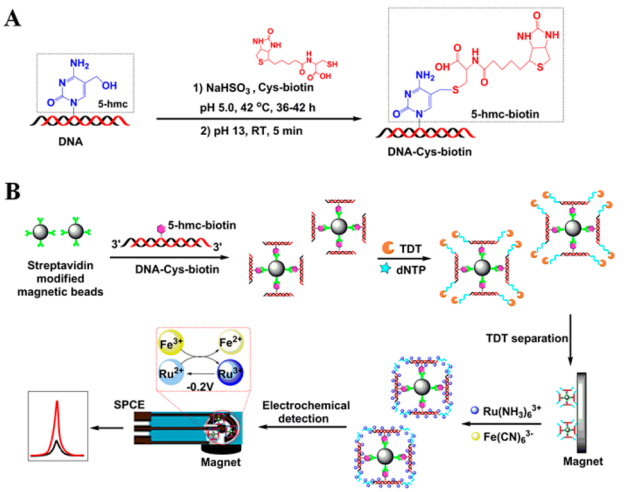

[a]This assay involves two consecutive steps: (A) single-step bisulfite-mediated biotinylation of 5-hmC site in DNA; (B) dual signal amplification strategy for biotinylated 5-hmC DNA-induced TdT-catalyzed polymerization and subsequent Ru(III) redox recycling-mediated amplification.

DNA leads to the formation of a dsDNA, and the subsequent introduction of a biotinyl−cysteine derivative enables a single-step incorporation of biotin into the dsDNA at the 5-hmC site (Scheme 1A, the reaction mechanism for the modification of 5-hmC by the biotinyl−cysteine derivative is shown in Figure S1). After the removal of excess Cys−biotins and salts using a Micro-Bio-Spin P6 column, the biotinylated dsDNAs are enriched by using the streptavidin-coated magnetic bead (MB) through specific biotin−streptavidin interaction (Scheme 1B). Subsequently, the 3′-hydroxy termini of DNA may be extended by TDT that catalyzes the repetitive addition of dNTPs without the requirement of any DNA templates, generating a longer DNA sequence. In this electrocatalytic reporter system, $Ru(NH_3)_6^{3+}$ functions as a primary electron acceptor, and $Fe(CN)_6^{3-}$ acts as a secondary electron acceptor. The $Ru(NH_3)_6^{3+}$ may be electrostatically attracted to the negatively charged phosphate backbone of DNAs on the surface of MB and immobilized on the SPCE electrode with the assistance of a magnetic field. The excess of $Fe(CN)_6^{3-}$ may amplify the current flowing to $Ru(NH_3)_6^{3+}$ by chemically oxidizing the electrochemically reduced Ru(II), resulting in the recycling of Ru(III) and the generation of an amplified electrocatalytic current. The electrocatalytic cycle follows an electron transfer kinetic-based mechanism[29] described by eqs 1 and 2.

$$Ru(NH_3)_6^{3+} + e^- \rightarrow Ru(NH_3)_6^{2+} \quad (1)$$

$$Ru(NH_3)_6^{2+} + Fe(CN)_6^{3-} \rightarrow Ru(NH_3)_6^{3+} + Fe(CN)_6^{4-} \quad (2)$$

This $Ru(NH_3)_6^{3+}/Fe(CN)_6^{3-}$ system may generate an enhanced electrocatalytic signal once the biotinylated 5-hmC DNA binds to MB on the SPCE. Moreover, $Fe(CN)_6^{3-}$ is negatively charged and cannot access the surface of the electrode which is masked by the partially anionic DNA, eliminating their direct reaction for false-positive signal. Due to the extremely specific 5-hmC-induced single-step biotinylation reaction and highly efficient dual signal amplification between TdT-catalyzed polymerization reaction and Ru(III) redox recycling-mediated amplification, this biosensor enables simple, rapid, and selective detection of 5-hmC with ultrahigh sensitivity.

The preparation of electrochemical magnetoelectrochemical biosensor is characterized by electrochemical impedance spectroscopy (EIS) and zeta potential (Figure 1). The electron-transfer resistance (R_{et}) is controlled by the electron

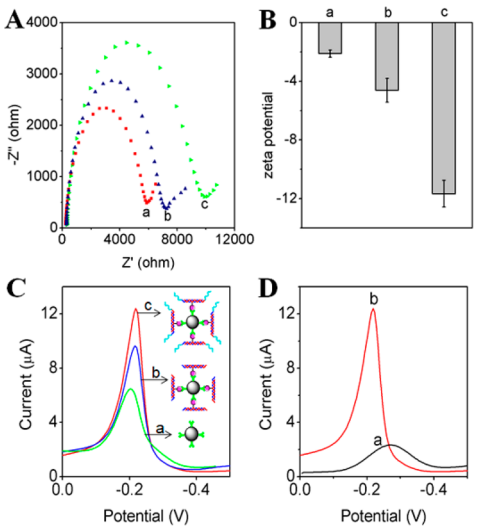

Figure 1. (A) Nyquist plots of electrochemical impedance spectroscopy (EIS) of MB/SPCE (a) and biotinylated 5-hmC DNA/MB/SPCE before (b) and after (c) TdT-assisted base extension in 5 mM $Fe(CN)_6^{3-/4-}$ solution containing 0.1 M KCl. (B) Zeta potential of MB (a) and biotinylated 5-hmC DNA/MB before (b) and after (c) TdT-assisted base extension. (C) DPV responses of MB/SPCE (a) and biotinylated 5-hmC DNA/MB/SPCE before (b) and after (c) TdT-assisted base extension in the mixture of $Ru(NH_3)_6^{3+}$ and $Fe(CN)_6^{3-}$. (D) DPV signal of the biotinylated 5-hmC DNA/MB/SPCE and the subsequent TdT-assisted base extension in the presence of (a) $Ru(NH_3)_6^{3+}$ only and (b) $Ru(NH_3)_6^{3+}$ and $Fe(CN)_6^{3-}$.

DOI: 10.1021/acs.analchem.8b04663
Anal. Chem. XXXX, XXX, XXX−XXX

transfer kinetics of $[Fe(CN)_6]^{3-/4-}$ on different SPCE and may be characterized by the semicircle diameter of the Nyquist plot. As shown in Figure 1A, the immobilization of MB on SPCE displays a semicircle diameter with a R_{et} of 5980 Ω (Figure 1A, curve a). In contrast, biotinylated 5-hmC DNA/MB exhibits a larger R_{et} of 7120 Ω (Figure 1A, curve b) due to the electrostatic repulsion effect between the negatively charged DNA and $Fe(CN)_6^{3-/4-}$, indicating the successful modification of 5-hmC DNA on the MB. After the incubation of biotinylated 5-hmC DNA with TDT, the R_{et} increases to 9980 Ω. This may be explained by the fact that, after TdT-catalyzed polymerization, a more negatively charged phosphoric acid backbone of biotinylated 5-hmC DNA may hinder the electron transfer of $[Fe(CN)_6]^{3-/4-}$ from solution to the electrode surface (Figure 1A, curve c).

The zeta potential is used to investigate the linking of biotinylated 5-hmC on MB. As shown in Figure 1B, the addition of biotinylated 5-hmC DNA induces a significant change in zeta potential (Figure 1B, curve b, −4.5 ± 0.2 mV) compared with the control group with only MB (Figure 1B, curve a, −2.3 ± 0.5 mV), indicating the successful coating of biotinylated 5-hmC DNA onto the MB surface. When the 5-hmC DNA is incubated with TDT, a higher negative zeta potential (−10.2 ± 0.4 mV) is observed (Figure 1B, curve c) due to the biotinylated 5-hmC DNA-induced TdT-catalyzed polymerization.

DPV measurements are recorded using different electrodes including MB/SPCE and biotinylated 5-hmC DNA/MB/SPCE before and after TdT-assisted base extension in the mixture of $Ru(NH_3)_6^{3+}$ and $Fe(CN)_6^{3-}$ (Figure 1C). In the control group without the 5-hmC site in DNA, the current is small (5.59 μA) (Figure 1C, curve a). After the biotinylation of the 5-hmC site in DNA, the signal increases to 7.85 μA (Figure 1C, curve b) due to the absorption of abundant $Ru(NH_3)_6^{3+}$ onto the negatively charged phosphate backbone of biotinylated 5-hmC DNA. After the incubation of the biotinylated 5-hmC DNA/MB with TDT, the signal further increases to 11.5 μA (Figure 1C, curve c), because more $Ru(NH_3)_6^{3+}$ is electrostatically bound to the negatively charged phosphate backbone of the extended 5-hmC DNA. These results demonstrate the feasibility of this biosensor for the 5-hmC assay.

To study the effect of oxidant $Fe(CN)_6^{3-}$ upon the cathodic current signal, we compared the DPV signal of the biotinylated 5-hmC DNA/MB/SPCE and the subsequent TdT-assisted base extension before and after the addition of $Fe(CN)_6^{3-}$. The electrochemical signal can be amplified by the recycling of Ru(III) redox that binds to the negatively charged phosphate backbone of DNAs by electrostatic interactions. Specifically, the $Ru(NH_3)_6^{3+}$ that is reduced to $Ru(NH_3)_6^{2+}$ at the electrode surface can be chemically oxidized back to $Ru(NH_3)_6^{3+}$ by $Fe(CN)_6^{3-}$, leading to the recycling of Ru(III) for the generation of an amplified electrocatalytic current. As shown in Figure 1D, DPV current (I_a) of the magnetobiosensor in the presence of $Ru(NH_3)_6^{3+}$ without $Fe(CN)_6^{3-}$ is 1.603 μA, while the DPV current (I_b) of the magnetobiosensor in the presence of $Ru(NH_3)_6^{3+}$and $Fe(CN)_6^{3-}$ is 11.5 μA. The increment of the peak current ($\Delta I = I_b - I_a$) is 9.9 μA, indicating that the DPV signals of $Ru(NH_3)_6^{3+}$ and $Fe(CN)_6^{3-}$ (Figure 1D, curve b) are amplified approximately 10-fold over that of only $Ru(NH_3)_6^{3+}$ redox (Figure 1D, curve a).

Under the optimal experimental conditions (see Figures S2 and S3), we evaluated the analytical performance of the magnetoelectrochemical biosensor in response to different concentrations of 5-hmC DNA. As shown in Figure 2A, the

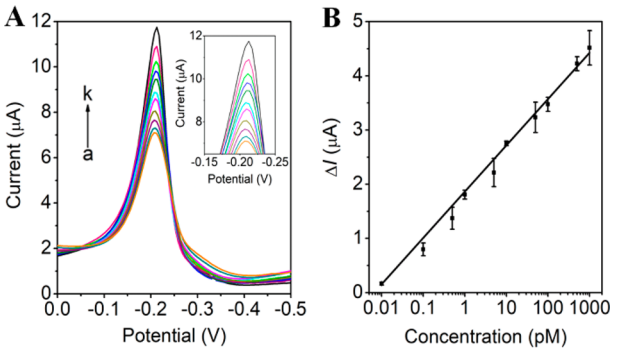

Figure 2. (A) DPV response of the electrochemical magnetobiosensor to different concentrations of 5-hmC DNA (from a to k: 0, 0.01, 0.1, 0.5, 1, 5, 10, 50, 100, 500, and 1000 pM). Inset shows the enlarged DPV current curve. (B) The linear relationship between the DPV peak current enhancement (ΔI) and the logarithm of 5-hmC concentration in the range from 0.01 to 1000 pM. The error bars represent the standard deviation of three repetitive measurements.

DPV signal enhances with the increasing concentration of 5-hmC DNA from 0.01 to 1000 pM. A linear relationship is obtained between the current and the logarithm of 5-hmC DNA concentration in the range from 0.01 to 1000 pM (Figure 2B), and the correlation equation is ΔI (μA) = 0.8540 $\log_{10} C$ + 1.864 (R^2 = 0.9978), where C (pM) is the concentration of 5-hmC DNA and ΔI is the signal enhancement ($\Delta I = I - I_0$, where I_0 and I are the DPV currents of the biosensor in the absence and presence of 5-hmC DNA, respectively). The detection limit is calculated to be 9.06 fM. The sensitivity of this biosensor has improved by 4 orders of magnitude than that of the DNA methyltransferase modification-based electrochemical assay (0.23 nM),[30] 4 orders of magnitude than that of the β-glucosyltransferase modification-based fluorescent assay (0.167 nM),[31] 46-fold than that of the 5-hmC specific antibodies-based optical sensor (0.42 pM),[32] and 15-fold than that of the 5-hmC selective chemical oxidation by $KRuO_4$-based electrogenerated chemiluminescence assay (0.14 pM).[24] The high sensitivity of this biosensor may be ascribed to (1) the specific biotinylation of the 5-hmC site in DNA by biotinyl−cysteine, (2) the high efficiency of TdT-mediated polymerization, and (3) the signal amplification induced by the reduction of Ru(III) at the electrode surface and the subsequent reoxidization by excess Fe(III).

To investigate the specificity of this biosensor, we used the 5-mC DNA with one 5-mC site (5-methylcytosine, 5-mC) and normal DNA (cytosine, C) for comparison. As shown in Figure 3A, the reaction of the 5-hydroxy group of 5-hmC with bisulfite forms a sulfite ester that subsequently undergoes the substitution by a nucleophilic thiolate, resulting in the incorporation of biotin into 5-hmC DNA at the 5-hmC site. However, under the identical conditions, C and 5-mC (as the nucleosides) cannot make the incorporation of biotin into the DNA. A peak current of 11.5 μA is observed in response to 5-hmC DNA. In contrast, a low peak current of 5.76 and 5.607 μA is observed, respectively, in response to the normal DNA and 5-mC DNA even at 10-fold higher concentration than 5-hmC DNA (0.1 nM vs 1 nM) (Figure 3B), with peak current

DOI: 10.1021/acs.analchem.8b04663
Anal. Chem. XXXX, XXX, XXX−XXX

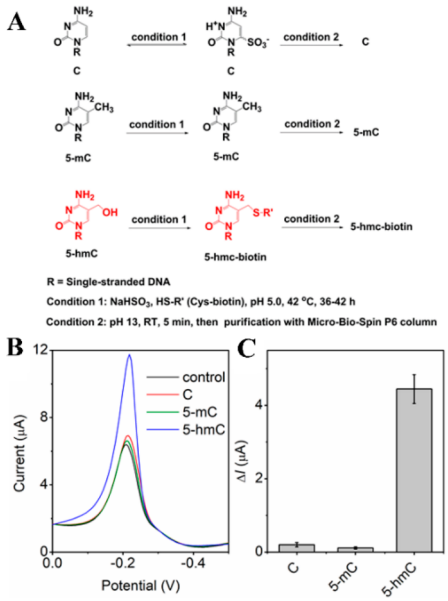

Figure 3. (A) 5-hmC is converted into 5-hmC−biotin under condition 1, and it is purified with Micro-Bio-Spin P6 under condition 2; however, C and 5-mC cannot make the incorporation of biotin into the DNA under conditions 1 and 2. (B) DPV curves of the electrochemical magnetobiosensor and (C) variance of the DPV signal in response to the control group with only reaction buffer, normal DNA (C), 5-mC DNA (5-mC), and 5-hmC DNA (5-hmC), respectively. Error bars represent the standard deviation from three independent experiments.

change (ΔI) of 5-hmC being 22−39-fold higher than those of the normal DNA and 5-mC DNA (Figure 3C), suggesting the high specificity of this biosensor toward 5-hmC. The high specificity may be ascribed to the chemical reaction of 5-hmC modification not being able to happen at any other unhydroxymethylated nucleic acid bases.[25]

To assess the stability of the biosensor, a batch of magnetoelectrochemical biosensors is stored at 4 °C and measured over a period of 7 days. As shown in Figure S4, no significant change in the peak current is observed during 7 days, and only a 4.6% decrease in the peak current is observed after storing in the refrigerator at 4 °C for 3 weeks, demonstrating the excellent stability of this biosensor. We further examined the intraassay and interassay precision of the proposed biosensor. The relative standard deviation (RSD) for ten measurements of 100 pM 5-hmC with the same biosensor under identical conditions is 3.5%, while the RSD for six parallel measurements using six biosensors fabricated with the same process is 2.5%, indicating good reproducibility of this biosensor.

The 5-hmC levels are extremely low in cancer cells,[33] suggesting that a lack of 5hmC may become a useful biomarker for cancer diagnosis. To evaluate the feasibility of the proposed biosensor in clinical diagnosis, we used this biosensor to measure two different cancer cell lines including the human cervical carcinoma cell line (HeLa cells) and embryonic kidney cell line (HEK 293T cells). The concentration of genomic DNA is measured by a Q-5000 UltramicroUV-Vis spectrophotometer (Quawell, USA). As shown in Figure 4, the 5-hmC level of HeLa cells and HEK 293T cells is determined to be 0.00793% and 0.00977% of the total nucleotides, respectively, consistent with the previous report obtained by the β-

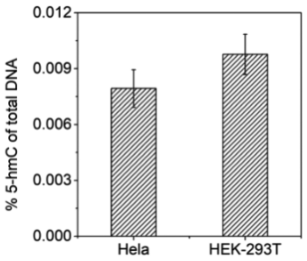

Figure 4. Quantification of the 5-hmC site in genomic DNA isolated from HeLa cells and HEK 293T cells. Error bars represent the standard deviation from three independent experiments.

glucosyltransferase modification-based dot-blot assay (0.007% and 0.009% of total nucleotides, respectively).[34] In addition, we measured the serum samples spiked with 5-hmC DNA. The recoveries are measured to be in the range of 98.5−104.0% with a RSD of 2.3−3.3% (see Table S2), indicating that our method possesses good accuracy even in complex media.

In summary, we have developed a label-free and immobilization-free electrochemical magnetobiosensor for sensitive detection of 5-hmC in genomic DNA based on a dual signal amplification strategy coupled with TDT-assisted enzymatic amplification and Ru(III) redox cycling. This biosensor has several unique merits: (1) TdT can directly extend DNA strands along the 3′ OH terminal of DNA without the requirement of either DNA templates or special design of specific restriction enzyme recognition sequences; (2) the small redox $Ru(NH_3)_6^{3+}$ electrostatically binds to the DNA sequence, which can quantitatively reflect the extended DNA and the concomitant amplified signals, without the involvement of the labeling of DNA by redox molecules; (3) the Ru(III) is reduced at the electrode surface and subsequently reoxidized by excess Fe(III), significantly amplify the current signal; (4) this biosensor can discriminate three major epigenetic structural variants within DNA bases including cytosine, 5-methylcytosine, and 5-hydroxymethylcytosine. This biosensor may find wide applications in the study of the 5-hmC methylation/demethylation mechanism and the clinical diagnosis of epigenetic-associated diseases.

■ ASSOCIATED CONTENT

Supporting Information

The Supporting Information is available free of charge on the ACS Publications website at DOI: 10.1021/acs.analchem.8b04663.

Four figures and two tables showing the reaction mechanism, optimization of experimental conditions, comparison of assay performance between different sizes of magnetic beads, stability and reproducibility of the magnetoelectrochemical biosensor, oligonucleotide sequence information, and recovery study in diluted serum samples (PDF)

■ AUTHOR INFORMATION

Corresponding Author

*Tel.: +86 0531-86186033. Fax: +86 0531-82615258. E-mail: cyzhang@sdnu.edu.cn.

ORCID

Chun-yang Zhang: 0000-0002-8010-1981

DOI: 10.1021/acs.analchem.8b04663
Anal. Chem. XXXX, XXX, XXX−XXX

Author Contributions

‡L.C., J.H., M.W., and C.L. contributed equally.

Notes

The authors declare no competing financial interest.

■ ACKNOWLEDGMENTS

This work was supported by the National Natural Science Foundation of China (Grant Nos. 21527811, 21605096, and 21575152) and the Award for Team Leader Program of Taishan Scholars of Shandong Province, China.

■ REFERENCES

(1) Egger, G.; Liang, G.; Aparicio, A.; Jones, P. A. *Nature* **2004**, *429*, 457−463.
(2) Khare, T.; Pai, S.; Koncevicius, K.; Pal, M.; Kriukiene, E.; Liutkeviciute, Z.; Irimia, M.; Jia, P.; Ptak, C.; Xia, M.; Tice, R.; Tochigi, M.; Morera, S.; Nazarians, A.; Belsham, D.; Wong, A. H. C.; Blencowe, B. J.; Wang, S. C.; Kapranov, P.; Kustra, R.; Labrie, V.; Klimasauskas, S.; Petronis, A. *Nat. Struct. Mol. Biol.* **2012**, *19*, 1037−1043.
(3) Muenzel, M.; Globisch, D.; Brueckl, T.; Wagner, M.; Welzmiller, V.; Michalakis, S.; Mueller, M.; Biel, M.; Carell, T. *Angew. Chem., Int. Ed.* **2010**, *49*, 5375−5377.
(4) Kriukiene, E.; Liutkeviciute, Z.; Klimasauskas, S. *Chem. Soc. Rev.* **2012**, *41*, 6916−6930.
(5) Tahiliani, M.; Koh, K. P.; Shen, Y.; Pastor, W. A.; Bandukwala, H.; Brudno, Y.; Agarwal, S.; Iyer, L. M.; Liu, D. R.; Aravind, L.; Rao, A. *Science* **2009**, *324*, 930−935.
(6) Zhang, L.; Chen, W.; Iyer, L. M.; Hu, J.; Wang, G.; Fu, Y.; Yu, M.; Dai, Q.; Aravind, L.; He, C. *J. Am. Chem. Soc.* **2014**, *136*, 4801−4804.
(7) Ladwein, K. I.; Jung, M. *Angew. Chem., Int. Ed.* **2011**, *50*, 12143−12145.
(8) Crawford, D. J.; Liu, M. Y.; Nabel, C. S.; Cao, X.-J.; Garcia, B. A.; Kohli, R. M. *J. Am. Chem. Soc.* **2016**, *138*, 730−733.
(9) Nestor, C.; Ruzov, A.; Meehan, R. R.; Dunican, D. S. *BioTechniques* **2010**, *48*, 317−319.
(10) Song, C.-X.; Clark, T. A.; Lu, X.-Y.; Kislyuk, A.; Dai, Q.; Turner, S. W.; He, C.; Korlach, J. *Nat. Methods* **2012**, *9*, 75−77.
(11) Tang, Y.; Zheng, S.-J.; Qi, C.-B.; Feng, Y.-Q.; Yuan, B.-F. *Anal. Chem.* **2015**, *87*, 3445−3452.
(12) Ito, S.; D'Alessio, A. C.; Taranova, O. V.; Hong, K.; Sowers, L. C.; Zhang, Y. *Nature* **2010**, *466*, 1129−1133.
(13) Liutkeviciute, Z.; Kriukiene, E.; Grigaityte, I.; Masevicius, V.; Klimasauskas, S. *Angew. Chem., Int. Ed.* **2011**, *50*, 2090−2093.
(14) Szwagierczak, A.; Bultmann, S.; Schmidt, C. S.; Spada, F.; Leonhardt, H. *Nucleic Acids Res.* **2010**, *38*, No. e181.
(15) Nestor, C. E.; Ottaviano, R.; Reddington, J.; Sproul, D.; Reinhardt, D.; Dunican, D.; Katz, E.; Dixon, J. M.; Harrison, D. J.; Meehan, R. R. *Genome Res.* **2012**, *22*, 467−477.
(16) Zhong, S.; Li, Z.; Jiang, T.; Li, X.; Wang, H. *Anal. Chem.* **2017**, *89*, 5702−5706.
(17) Pastor, W. A.; Pape, U. J.; Huang, Y.; Henderson, H. R.; Lister, R.; Ko, M.; McLoughlin, E. M.; Brudno, Y.; Mahapatra, S.; Kapranov, P.; Tahiliani, M.; Daley, G. Q.; Liu, X. S.; Ecker, J. R.; Milos, P. M.; Agarwal, S.; Rao, A. *Nature* **2011**, *473*, 394−397.
(18) Chen, S.; Dou, Y.; Zhao, Z.; Li, F.; Su, J.; Fan, C.; Song, S. *Anal. Chem.* **2016**, *88*, 3476−3480.
(19) Wang, X.; Chen, F.; Zhang, D.; Zhao, Y.; Wei, J.; Wang, L.; Song, S.; Fan, C.; Zhao, Y. *Chem. Sci.* **2017**, *8*, 4764−4770.
(20) Chen, F.; Wang, X.; Cao, X.; Zhao, Y. *Anal. Chem.* **2017**, *89*, 10468−10473.
(21) Zhou, Y.; Yang, Z.; Li, X.; Wang, Y.; Yin, H.; Ai, S. *Electrochim. Acta* **2015**, *174*, 647−652.
(22) Hoebartner, C. *Angew. Chem., Int. Ed.* **2011**, *50*, 4268−4270.
(23) Shahal, T.; Gilat, N.; Michaeli, Y.; Redy-Keisar, O.; Shabat, D.; Ebenstein, Y. *Anal. Chem.* **2014**, *86*, 8231−8237.
(24) Ma, S.; Sun, H.; Li, Y.; Qi, H.; Zheng, J. *Anal. Chem.* **2016**, *88*, 9934−9940.
(25) Li, W.-W.; Gong, L.; Bayley, H. *Angew. Chem., Int. Ed.* **2013**, *52*, 4350−4355.
(26) Wu, Q.; Amrutkar, S. M.; Shao, F. *Bioconjugate Chem.* **2018**, *29*, 245−249.
(27) Campuzano, S.; Torrente-Rodriguez, R. M.; Lopez-Hernandez, E.; Conzuelo, F.; Granados, R.; Sanchez-Puelles, J. M.; Pingarron, J. M. *Angew. Chem., Int. Ed.* **2014**, *53*, 6168−6171.
(28) Chen, Y.; Xianyu, Y.; Dong, M.; Zhang, J.; Zheng, W.; Qian, Z.; Jiang, X. *Anal. Chem.* **2018**, *90*, 6906−6912.
(29) Gasparac, R.; Taft, B. J.; Lapierre-Devlin, M. A.; Lazareck, A. D.; Xu, J. M.; Kelley, S. O. *J. Am. Chem. Soc.* **2004**, *126*, 12270−12271.
(30) Jiang, W.; Lu, Y.; Wang, H.; Wang, M.; Yin, H. *Microchim. Acta* **2017**, *184*, 3789−3796.
(31) Chen, H.-y.; Wei, J.-R.; Pan, J.-X.; Zhang, W.; Dang, F.-q.; Zhang, Z.-Q.; Zhang, J. *Biosens. Bioelectron.* **2017**, *91*, 328−333.
(32) Hawk, R. M.; Armani, A. M. *Biosens. Bioelectron.* **2015**, *65*, 198−203.
(33) Kafer, G. R.; Li, X.; Horii, T.; Suetake, I.; Tajima, S.; Hatada, I.; Carlton, P. M. *Cell Rep.* **2016**, *14*, 1283−1292.
(34) Song, C.-X.; Szulwach, K. E.; Fu, Y.; Dai, Q.; Yi, C.; Li, X.; Li, Y.; Chen, C.-H.; Zhang, W.; Jian, X.; Wang, J.; Zhang, L.; Looney, T. J.; Zhang, B.; Godley, L. A.; Hicks, L. M.; Lahn, B. T.; Jin, P.; He, C. *Nat. Biotechnol.* **2011**, *29*, 68−72.

DOI: 10.1021/acs.analchem.8b04663
Anal. Chem. XXXX, XXX, XXX−XXX